

Fission Characteristics of Heavy Nuclei: Statics and Dynamics

Birger B. Back

Argonne National Laboratory
Argonne, IL 60439, U.S.A.

Received 1 January 1999

Abstract. This paper presents a selective historical perspective of fission research over the last thirty-five years while Ray Nix has made central contributions to the field. The emphasis is placed on early studies of the shell stabilized secondary minimum in the static fission barrier and on the dynamic properties of fission of hot nuclei, which have recently been the focus of intense study.

Keywords: Fission, Shell corrections, double humped barrier, fission dynamics, nuclear viscosity

PACS: 25.70Jj

1. Introduction

Ray Nix's contributions to nuclear fission research span his whole career and a wide range of topics. As the title indicates, these include both the static properties of fissioning systems, such as the potential energy surface as a function of various shape parameters, as well as the dynamic aspects of fission, which traditionally has been studied in terms of the kinetic energy release. Recently it has, however, become possible to measure the time scale of fission and learn about the effects of friction or viscosity of nuclei undergoing large shape changes.

In this talk I would like to review just a few of these topics which are selected only on the basis that they overlapped with my own work.

2. The double-humped fission barrier

In the late sixties, there was much excitement in the field of nuclear fission research when it was realized that several puzzling experimental results found a consistent ex-

planation [1] in terms of a secondary minimum in the fission barrier. This is caused by the shell stabilization at large deformation with an axis ratio of 2:1 of axially symmetric prolate deformation. The experimental evidence included the observation of anomalously short-lived fission activities in the bombardment of ^{238}U with beams of ^{22}Ne and ^{16}O [2], the observation of an enhanced fission decay width at intervals of about 650 eV in slow neutron induced fission of ^{240}Pu [3] as well as gross resonances in the $^{230}\text{Th}(n,f)$ [4], $^{233,235}\text{U}(d,pf)$ and $^{239,241}\text{Pu}(d,pf)$ [5] reactions. Realizing that the fission barrier in actinide nuclei typically is double-humped, these observations were naturally explained as manifestations of spontaneous fission of nuclei trapped in the super-deformed minimum and the enhancements in the fission decay width afforded by the coupling to compound states and ‘ β ’-vibrational resonances in the second well, respectively. In fact, the vibrational resonance in the fission excitation function of $^{239}\text{Pu}(d,pf)$ is clearly observed in a decade earlier experiment by Northrop, Stokes, and Boyer [6], but it was mis-interpreted as a plateau created by a wide gap between the lowest fission channels.

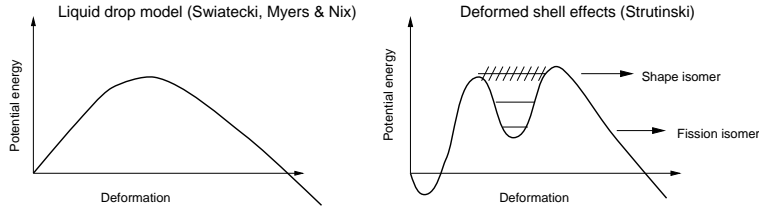


Fig. 1. The liquid drop fission barrier [7] (top panel) is modified by the deformation dependence if the single particle shell structure [8]. The double-humped potential gives rise to short-lived fission isomers and shape resonances as discussed in the text.

With the double-humped barrier well established in the actinide region it quickly became clear that further detailed analysis of data required fast and reliable algorithms for calculating the quantum mechanical tunneling through this complex barrier. Different parameterizations of the double-humped shape were studied and both analytical [9] and numerical [10] solutions to the quantum-mechanical tunneling problem were found. Cramer and Nix proposed [9] a parameterization in terms of three smoothly joined parabolas, which has a sufficient number of parameters to describe the essential characteristics of the deformation path and was associated with a relatively simple analytical solution to the tunneling problem.

These calculations all showed the peaks in the tunneling probability associated with vibrational states in the second well, but it soon became clear that the large observed width of the resonances could not be reproduced [11]. Bondorf had pointed out, however, that this is a manifestation of the coupling between the purely vibrational states and the much more abundant compound states in the second well, and

that this effect can be included by introducing an absorptive imaginary potential [10].

Having arrived at Los Alamos in the spring of 1971 to work with Chip Britt, I wanted to analyze our fission probability data with this resonance structure using Ray's method but needed to include the imaginary potential to correctly reproduce the observed resonance widths.

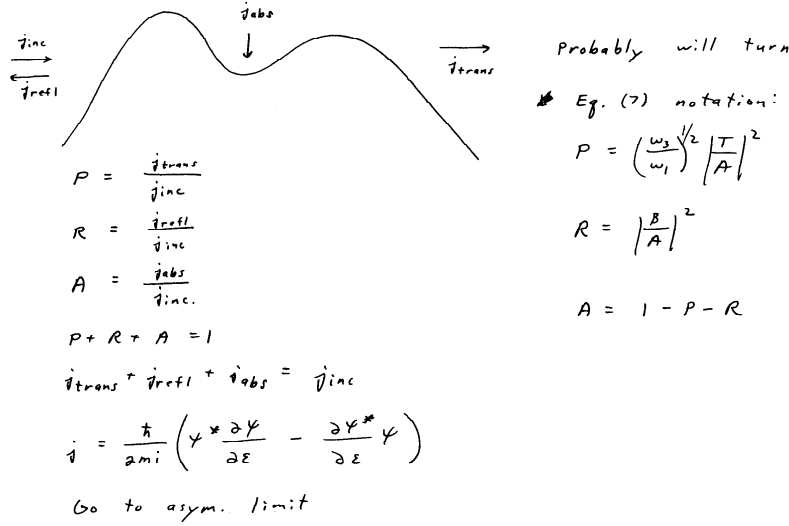


Fig. 2. Notes on the calculation of the transmission through the double-humped barrier in the presence an absorptive negative imaginary potential in the second well [12]

Attempting to consult with Ray on this topic I went to his office. Initially I thought that it was vacant - the desktop was clean, without the normal stacks of books and papers, but upon closer inspection I discovered one open book on the desk and neatly arranged ring binders and books on the shelves. Later I learned that this was quite normal. I also managed to talk to Ray about the problem of absorption in the second well and soon received the note shown in Fig. 1, which indicates how the solution can be obtained.

An example of fission probability data is shown in Fig. 3 for the $^{230,232}\text{Th}(t, pf)$ reactions [13]. Strong vibrational resonances are clearly visible - in particular in the the $^{232}\text{Th}(t, pf)$ reaction - and the data are quite well reproduced within the model calculations. A large number of nuclei in the actinide region were studied in this manner and from the analysis it was possible to determine the heights of both the inner and outer barriers, when combined with an analysis of fission isomer excitation functions and half-lives [14]. The systematics of the fission barriers heights for even-even isotopes of Th, U, Pu and Cm obtained in this manner is shown in Fig. 4 .

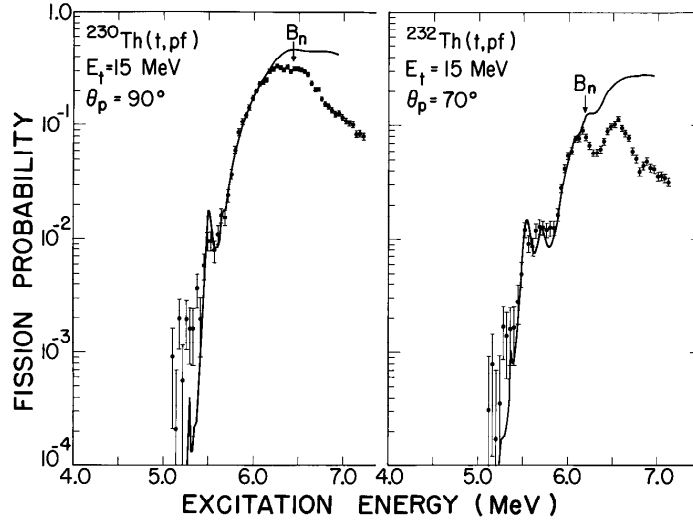


Fig. 3. Fission probability for the $^{230,232}\text{Th}(t,pf)$ -reactions [13].

We observe that the inner barrier height, E_A (top panels) is rather constant over this range of nuclei whereas the outer barrier height E_B (bottom panels) falls off with atomic number of the fissioning system.

The solid and dash-dotted lines are calculations by Möller and Nix [15] using a folded Yukawa and a modified harmonic oscillator potential, respectively, whereas the dotted curve was obtained with a Woods-Saxon potential by Pauli and Ledergerber [16]. The most striking discrepancy between the data and calculations is seen for the inner barrier in Th. It has later been verified that this discrepancy is only apparent because the barrier heights obtained from the fission probability data are in fact those of a double peaked outer barrier; the inner barrier has not yet been measured and may well be as low as predicted.

3. Fission dynamics - time-scales

For many years, the empirical information on fission dynamics was obtained almost exclusively from studies of the total kinetic energy (TKE) release in fission. This quantity was shown to follow a fairly simple systematics [17], with an approximately linear dependence on the parameter $Z^2/A^{1/3}$, which scales with the Coulomb repulsion between the nascent fragments at scission. A linear scaling between TKE and $Z^2/A^{1/3}$ is obtained if one assumes that 1) the system is essentially stationary at scission and 2) that the overall shape (charge distribution) is independent of the size of the system. However, as shown by Davies, Sierk, and Nix [18] these

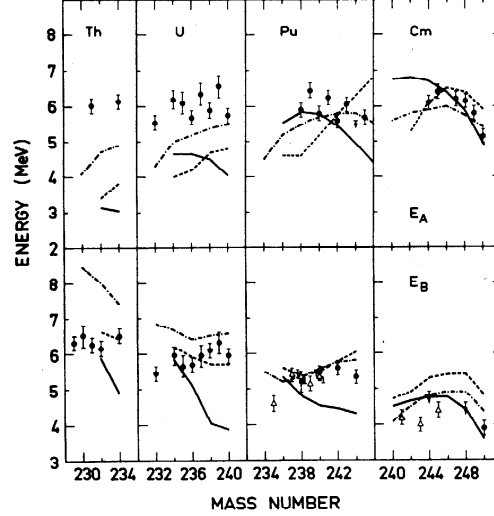


Fig. 4. Experimental fission barrier heights for even-even Th, U, Pu, and Cm isotopes [13] (solid circles) [14] (open triangles) are compared to Strutinski-type calculations using a folded Yukawa (solid curves) [15], a modified harmonic oscillator (dashed-dotted curves) [15], and a Woods-Saxon potential (dotted curves) [16].

conditions are not necessarily fulfilled in realistic dynamical calculations within the liquid drop model incorporating a viscosity term. They found, however, that for a viscosity of $\eta = 0.015$ TP (tera poise) (water has a viscosity of about $\eta \sim 0.01$ P at room temperature) could account well for the total kinetic energies over the range of available data.

3.1. Pre-scission neutron and γ -ray emission

In a set of pioneering experiments by Gavron *et al.* [19], and later by Hinde *et al.* [21], it was found that the multiplicity of neutrons emitted prior to scission in hot nuclei was substantially larger than expected for the time-scales for saddle-to-scission motion of $t_{ss} = 3.5 \times 10^{-21}$ seconds predicted by these dynamical calculation. This is illustrated in Fig. 5a and 5b, where the observed (open circles) pre-scission neutron multiplicity, ν_{pre} , exceeds the prediction from a purely statistical decay model (dashed curves); the short saddle-to-scission time of $t_{ss} = 3.5 \times 10^{-21}$ seconds would allow only for the additional emission of a fraction of a neutron during the descent from saddle to scission. Also the pre-scission emission of γ -rays in the Giant Dipole Resonance region (low energy component) of $E_\gamma = 9$ -13 MeV is seen to exceed the expectation from the statistical model (Fig. 5c). This also manifests itself in an enhanced angular anisotropy of γ -ray emission relative to the normal of

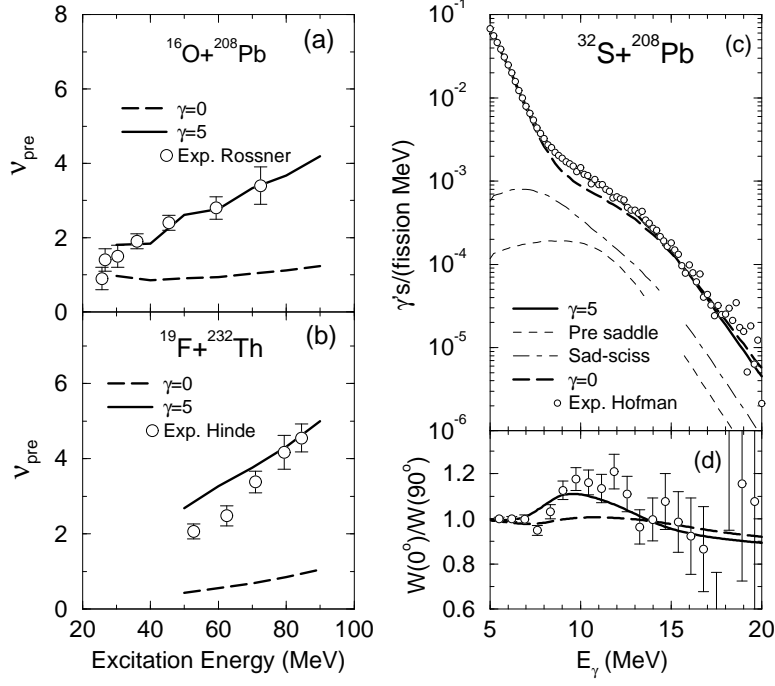


Fig. 5. Pre-scission neutron multiplicities (open circles) for the (a) $^{16}\text{O} + ^{208}\text{Pb}$ [20] and (b) $^{19}\text{F} + ^{232}\text{Th}$ [21] reactions are compared to statistical model calculations with (solid line) and without (dashed line) dissipation. The γ -ray spectrum (c) and anisotropy (d) in coincidence with fission fragments [22] are compared to statistical model calculations.

the reaction plane containing the two fission fragments, as illustrated in Fig 5d.

The full drawn curves in Fig. 5 all represent calculations which include the effects of dissipation in the fission process. Instead of counting up transition states at the fission saddle point, which leads to the standard Bohr-Wheeler [23] expression for the fission decay width, we have here used an expression based on a diffusion picture for the fission originally proposed by H. A. Kramers [24]. The fission decay width is thus assumed to be given by

$$\Gamma_f(t) = \Gamma_f^{BW} \{1 - \exp(-t/\tau_D)\} \{\sqrt{1 + \gamma^2} - \gamma\}, \quad (1)$$

where the factor $\{1 - \exp(-t/\tau_D)\}$ takes into account the fact that the buildup in fission flux over the saddle point occurs over a period of τ_D , whereas the factor $\{\sqrt{1 + \gamma^2} - \gamma\}$, the so-called Kramers factor, represents the reduction in the asymptotic fission width caused by dissipation. The normalized linear friction coefficient $\gamma = \beta/2\omega_0$ is given in terms of the reduced dissipation coefficient, β , and the char-

acteristic frequency $\omega_0 \sim 1 \times 10^{21} s^{-1}$ associated with the curvature of the saddle point. In addition to the delay and reduction of the fission flux across the saddle point, the dissipation also lengthens the time, τ_{ss} , for the descent from saddle to scission according to the relation [25]

$$\tau_{ss} = \tau_{ss}^0 \{\sqrt{1 + \gamma^2} + \gamma\} \quad (2)$$

where τ_{ss}^0 is the saddle-to-scission time without dissipation in the system. For the calculations shown in Fig. 5 as solid curves, a value of $\gamma = 5$ was used, which is seen to account reasonably well for the observed pre-scission of neutrons and γ -rays. However, the data for the $^{19}\text{F} + ^{232}\text{Th}$ reaction gives a hint that the dissipation strength is somewhat weaker at the lower excitation energies.

3.2. Cross sections

It is also expected that the fission dissipation will have a substantial effect on the competition between fission and particle evaporation in the decay cascade of hot nuclei. This will manifest itself in the observed cross section for fission or evaporation residue formation. In Fig. 6 this effect is illustrated for three different experiments, namely the evaporation residue cross section for $^{32}\text{S} + ^{184}\text{W}$, the survival probability of Th-like nuclei formed in deep-inelastic collisions between 400 MeV ^{40}Ar and ^{232}Th , and the fission cross section for the $^3\text{He} + ^{208}\text{Pb}$ reaction.

We observe in Fig. 6a that the cross section for evaporation residues in $^{32}\text{S} + ^{184}\text{W}$ collisions [27] increase with beam energy contrary to the purely statistical model prediction of a decreasing excitation function illustrated by the long-dashed curve labelled $\gamma=0$. When a fixed dissipation strength of $\gamma=5$ is introduced, the predicted evaporation residue cross section is increased by a factor of ten (dashed-dotted curve labelled $\gamma=5$ in Fig. 6a). However, none of these calculations reproduce the increase in cross section with excitation energy, and it appears that a temperature (excitation energy) dependent dissipation is required by the data. This observation has been made earlier by Hofman *et al.* [29] on the basis of pre-scission γ -ray measurements at different beam energies. The solid curve labelled $\gamma(T)$ incorporates a temperature dependent dissipation strength of the form displayed in Fig. 7 (open triangles) and is seen to give a good account of the measurements.

A similar conclusion is drawn from an analysis of the survival probability of Th-like recoils from deep inelastic scattering shown in Fig. 6b. Here the probability for survival of the recoiling target-like reaction partner associated with detected Ar-isotopes is plotted as a function of excitation energy. The correspondence between the measured reaction Q-value and the excitation energy of the target-recoil is not straight forward and is discussed in more detail in Ref. [28]. We observe that the survival probability does not decrease as precipitously with excitation energy as predicted by the standard statistical model represented by the long-dashed curve labelled $\gamma=0$. On the contrary, a dissipation strength that increases with temperature (solid curve, $\gamma(T)$), as shown by the open squares in Fig. 7, is required in order to account for the observed survival probability (solid curve, $\gamma(T)$, Fig. 6b).

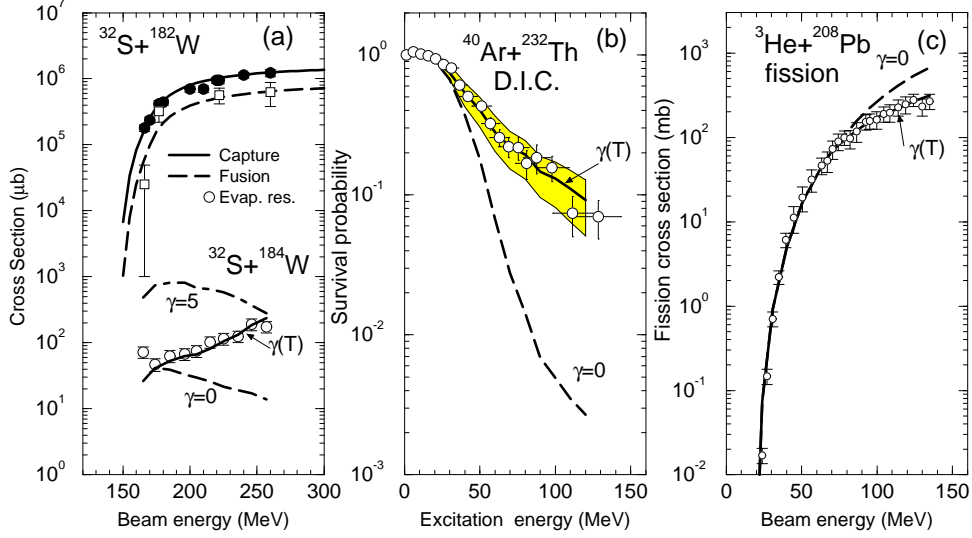


Fig. 6. Panel a: Evaporation residue cross sections for the $^{32}\text{S} + ^{184}\text{W}$ reaction (open circles) [27] is compared with statistical model calculations (see text). The fission (solid circles) and complete fusion (open squares) cross sections for $^{32}\text{S} + ^{182}\text{W}$ [26] are also shown. Panel b: The survival probability (open circles) of Th-like residues from the $^{40}\text{Ar} + ^{232}\text{Th}$ deep inelastic reaction at 400 MeV beam energy [28]. Panel c: Fission cross section for $^3\text{He} + ^{208}\text{Pb}$ [30].

Alternatively, it is equally instructive to analyze the fission cross section in a lighter system such as $^3\text{He} + ^{208}\text{Pb}$ [30], where fission is a relatively weak decay branch. We observe in Fig. 6c, that the measured fission cross section (open circles) does not increase as rapidly with beam energy as expected from the statistical model (long-dashed curve). Again, a dissipation strength which increases with excitation energy as shown by open circles in Fig. 7, is required to reproduce the measured cross section (solid curve, $\gamma(T)$, Fig. 6c).

The excitation energy dependence of the dissipation strength, γ , obtained from the above analysis is summarized in Fig. 7. Although it is clear that dissipation strengths increasing with temperature appears to be a general result from this analysis, it is interesting to note that the rate of increase varies strongly from system to system. The four systems studied here appear to divide into two pairs. The two Th-systems with masses of $A=226$ and $A\sim 232$ corresponding to neutron numbers of $N=134$, and ~ 142 exhibit a rapid increase in the dissipation strength above an excitation energy of ~ 40 MeV, whereas the ^{216}Th and ^{211}Po systems exhibit little or no dissipation up to an excitation energy of about 80 MeV followed by a gentle increase. The two latter systems have closed neutron shells ($N=126$ and $N=127$)

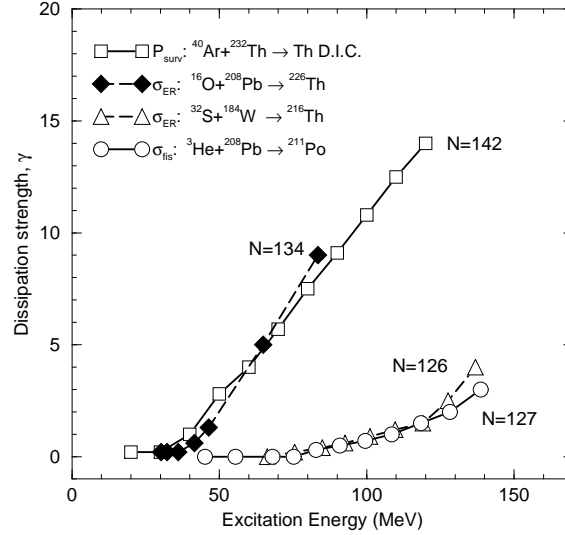


Fig. 7. Extracted dissipation strength derived from different experimental data

hinting at a dependence on the shell structure of the fissioning system. Thus, it appears that a closed nuclear shell structure suppresses the fission dissipation up to excitation energies of $E_{exc} \sim 80-100$ MeV, where the shell structure itself is dissolved. Admittedly, these conclusions are based in a very sparse data sample, and it would be very interesting to perform a more systematic study of these effects which spans a wider region with varying shell structure.

4. Conclusions

The continued interest in the fission process arises from the intricate relationship between the dynamics of large scale shape evolutions of a nuclear system and the underlying static properties. Over the last thirty-five years the study of this relationship has progressed very rapidly. In the early part of the period the research was concentrated on the static nuclear properties, such as the potential energy surface as a function of deformation. This focus was brought about by the the discovery of the complexity of the fission barrier and the many consequences this entailed for the fission properties of relatively cold nuclei. In the latter part of this period the studies shifted to fission of highly excited and/or rapidly rotating nuclei formed in reactions with heavy ion beams. In this talk I have focussed on a few of the many important contributions to this study that Ray Nix has made during his distinguished career in nuclear physics.

Acknowledgement

This work was carried out under the auspices of the U. S. Department of Energy under contract No. W-31-109-Eng38.

References

1. S. Bjornholm and V. M. Strutinski, Nucl. Phys. **A136** (1969) 1.
2. S. M. Polikanov, V. A. Druin, V. A. Karnaukov, V. L. Mikheev, A. A. Pleve, N. K. Skobelev, V. G. Subbotin, G. M. Ter-Akopyan, and V. A. Fomichev, J. Exptl. Theoret. Phys. (U.S.S.R.) **42** (1962) 1464; [Transl: Sov. Phys JETP, **15** (1962) 1016]
3. E. Migneco and J. P. Theobald, Nucl. Phys. **A112** (1968) 603.
4. P. E. Vorotnikov, S. M. Dubrovina, V. A. Shigin, and G. A. Otroschenko, Sov. J. Nucl. Phys. **5** (1967) 210.
5. J. Pederson and B. P. Kuzminov, Phys. Lett. **29B** (1969) 176; B. B. Back, J. P. Bondorf, G. A. Otroschenko, J. Pedersen, and B. Rasmussen, Nucl. Phys. **A165** (1971) 449.
6. J. A. Northrop, R. H. Stokes, and K. Boyer, Phys. Rev. **115** (1959) 1277.
7. J. R. Nix and W. Swiatecki, Nucl. Phys. **71** (1965) 1; W. D. Myers and W. Swiatecki, Nucl. Phys. **81** (1966) 1; J. R. Nix, Nucl. Phys. **A130** (1969) 241.
8. V. M. Strutinski, Nucl. Phys. **A95** (1967) 420; V. M. Strutinski, Nucl. Phys. **A122** (1968) 1.
9. J. D. Cramer and J. R. Nix, Phys. Rev. **C2** (1970) 1048; C. Y. Wong and J. Bang, Phys. Lett. **29B** (1969) 143.
10. J. P. Bondorf, Phys. Lett. **31B** (1970) 1.
11. B. B. Back, J. P. Bondorf, G. A. Otroschenko, J. Pedersen, and B. Rasmussen, Proc. of Physics and Chemistry of Fission, (IAEA, Vienna, 1969) p. 351;
12. Notes by Ray Nix given to me, June 1971.
13. B. B. Back, H. C. Britt, J. D. Garrett, and Ole Hansen, Phys. Rev. Lett. **28** (1972) 707.
14. H. C. Britt, M. Bolsterli, J. R. Nix, and J. L. Norton, Phys. Rev. **C7** (1973) 801.
15. P. Möller and J. R. Nix, in Proceedings of the Third International Conference on the Fission and Chemistry of Fission, Rochester, 1973, (IAEA, Vienna, 1974) p. 103.
16. H. C. Pauli and T. Ledergerber, Nucl. Phys. **A175** (1971) 545.
17. V. E. Viola, Jr. Nucl. Data, **1** (1966) 391.
18. K. T. R. Davies, A. Sierk, and J. R. Nix, Phys. Rev. **C13** (1976) 2385.
19. A. Gavron, J. Beene, B. Cheynis, R. L. Ferguson, F. E. Obershain, F. Plasil, G. R. Young, G. A. Petitt, M. Jääskeläinen, D. G. Sarantites, and C. F. Maguire, Phys. Rev. Lett. **47** (1981) 1255 [erratum: **48** (1982) 835]

-
20. H. Rossner, D. J. Hinde, J. R. Leigh, J. P. Lestone, J. O. Newton, J. X. Wei, and S. Elfström, Phys. Rev. **C45** (1992) 719.
 21. D. J. Hinde, R. J. Charity, G. S. Foote, J. R. Leigh, J. O. Newton, S. Ogaza, and A. Chattejee, Nucl. Phys. **A452** (1986) 550.
 22. D. J. Hofman, B. B. Back, I. Diószegi, C. P. Montoya, S. Schadmand, R. Varma, and P. Paul, Phys. Rev. Lett. **72** (1994) 470.
 23. N. Bohr and J. A. Wheeler, Phys. Rev. **56** (1939) 429.
 24. H. A. Kramers, Physica **7** (1940) 284.
 25. H. Hoffman and J. R. Nix, Phys. Lett **122B** (1983) 117.
 26. B. B. Back, P. B. Fernandez, B. G. Glagola, D. Henderson, S. Kaufman, J. G. Keller, S. J. Sanders, F. Videbaek, T. F. Tsang, and B. D. Wilkins, Phys. Rev. **C53** (1996) 1734.
 27. B. B. Back, D. J. Blumenthal, C. N. Davids, D. J. Henderson, R. Hermann, D. J. Hofman, C. L. Jiang, H. T. Penttilä, and A. H. Wuosmaa, To be published in Phys. Rev. **C** (1999)
 28. D. J. Hofman, B. B. Back, D. J. Henderson, V. Nanal, and A. H. Wuosmaa, Preprint (1999); see also B. B. Back, D. J. Blumenthal, C. N. Davids, D. J. Henderson, R. Hermann, D. J. Hofman, C. L. Jiang, H. T. Penttilä, and A. H. Wuosmaa, "Fission and Properties of Neutron-rich Nuclei", World Scientific, 1998, eds. Hamilton and Ramayya, p. 192.
 29. D. J. Hofman, B. B. Back, and P. Paul, Phys. Rev. **C51** (1995) 2597.
 30. Th. Rubehn, K. X. Jing, L. G. Moretto, L. Phair, K. Tso, and G. J. Wozniak, Phys. Rev. **C54** (1996) 3062.